

# Self-deflection of laser beams in a thin nonlinear film

G. A. Swartzlander, Jr., and A. E. Kaplan

Department of Electrical and Computer Engineering, The Johns Hopkins University, Baltimore, Maryland 21218

Received December 8, 1987; accepted December 8, 1987

The self-deflection of slab laser beams with right-triangular and semi-Gaussian intensity profiles that pass through a thin nonlinear film are compared, and semi-Gaussian beam profiles are found to produce near-maximum self-deflection angles. We also analyze symmetric profiles (both triangular and Gaussian), which, instead of self-(de)focusing, exhibit strongly counter-self-deflected beams in the far-field region. This evidence indicates that the self-deflection effect can dominate over self-focusing.

In earlier work<sup>1</sup> it was predicted that a beam of light with an asymmetric intensity profile incident upon a material with an intensity-dependent refractive index would have a curved trajectory. The effect was called self-bending or self-deflection. Consistent with this result,<sup>1</sup> this effect was observed experimentally<sup>2</sup> by using a pulsed ruby laser and a NaCl crystal as the nonlinear material. These effects may be understood readily from the following argument. When a beam of light with an asymmetric intensity profile, e.g., right triangular, propagates through a nonlinear medium, the wave fronts of the beam are retarded in proportion to the local intensity, thereby forming a light-induced prism in the beam path. Consequently, the beam follows a curved trajectory. The self-bending effect has potential in such applications as the fast angular scanning of laser beams,<sup>1</sup> the registration of superfast processes,<sup>3</sup> resonator-free optical bistability,<sup>4</sup> power limiting,<sup>5</sup> and the radiation protection of optical sensors.

If the optical path length through the nonlinear material is sufficiently long (as required to achieve nonlinear effects in materials with a small nonlinearity), then the initially asymmetric beam will suffer considerable distortions<sup>1</sup> of both the phase and intensity profiles, owing to diffraction and self-focusing effects.<sup>6</sup> From this point of view it is preferable to use a thin nonlinear layer to avoid these effects inside the nonlinear material. The geometric-optics treatment of self-focusing by a finite nonlinear layer was considered first in Ref. 7, and the diffractive theory of the external self-focusing in a nonlinear layer was developed in Ref. 8. Power limiting due to self-focusing in relatively thick nonlinear layers was observed in Ref. 9. Far-field effects were considered in Ref. 10, and external self-deflection was examined in Refs. 5 and 11.

Until recently, the possibility of using devices based on thin layers was limited since most of the available materials had relatively small nonlinearities. Fortunately, the emergence of new nonlinear-optical materials with large nonlinearities, such as superlattices and quantum-well structures,<sup>12</sup> direct-gap semiconductors,<sup>13</sup> liquid crystals,<sup>14</sup> artificial nonlinearities,<sup>15</sup> and doped glasses,<sup>16</sup> allows us to obtain considerable nonlinear effects even with a micrometer-sized layer of nonlinear material. These new materials create

more favorable conditions for experimental observations and applications of the self-bending effect. For example, the indication of the self-bending effect was observed in a liquid-crystal film<sup>17</sup> (there were insufficient data to permit us to compare our analysis with these results).

In this paper we calculate the self-bending due to a thin nonlinear film, basically concentrating on how this effect is affected by the shape of the spatial intensity profile of the beam, which is one of the most important issues in various applications of self-action effects. We consider single and adjacent right-triangular intensity profiles as well as semi-Gaussian and unobscured Gaussian intensity profiles. Surprisingly, the more realistic Gaussian beams give rise to nearly optimal self-deflection effects, indicating that the self-deflection effect is quite robust with respect to changes in the beam profile.

As a simple example, consider, as in Fig. 1, a beam propagating along the  $z$  axis and at normal incidence to a nonlinear film of thickness  $L$  whose refractive index depends on the intensity of light  $|E|^2$  as  $n = n_0 + n_2|E|^2$ . We assume that the electric field  $E$  does not vary in one of the transverse coordinates, e.g.,  $\partial E/\partial y = 0$ , that is, a slab or two-dimensional beam. The incident field (at  $z = 0$ ) can then be written as  $E(x, 0) = E_0(x)\exp[i\Phi_0(x)]$ . We will also assume that reflections at the interfaces and absorption within the film are negligible. In the linear region beyond the nonlinear film we use the paraxial approximation, treating only cases where the rays remain close to the optic axis. Finally, we assume that the film thickness is much shorter than both the diffraction length  $D$  and the self-focusing length  $R_{NL}$ ,<sup>6</sup> i.e.,

$$L \ll (D, R_{NL}),$$

where

$$D = kw^2/2, \\ R_{NL} = w(n_0/4n_2|E_m|^2)^{1/2}, \quad (1)$$

where  $|E_m|^2$  is the peak intensity of the incident beam and  $w$  is the characteristic beam size. This thinness requirement implies that only the phase (not the amplitude) of the transmitted beam is affected. The field at the transmitting interface can therefore be expressed as

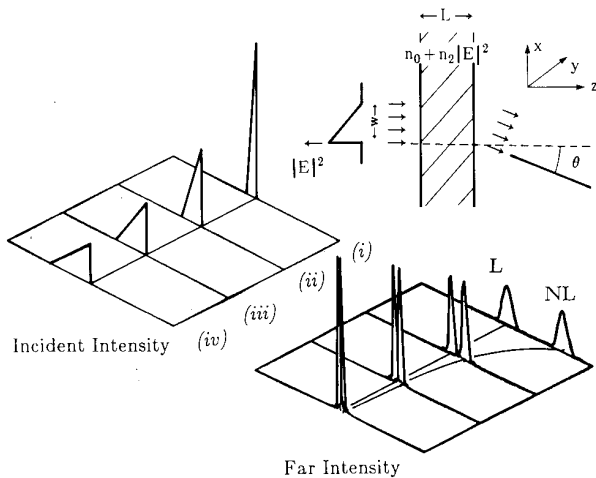


Fig. 1. Right-triangular incident intensity profiles of equal power ( $|E_m|^2 w_i/2 = \text{constant}$ ), with peak intensities  $|E_m|^2$  and beam size  $w_i$  (arbitrary units) varying, respectively, as (i) (1, 1), (ii) (1/2, 2), (iii) (1/3, 3), (iv) (1/4, 4). Their corresponding self-deflected beams are also shown. The deflected beams (NL) become resolved more clearly from their linear positions (L) as the beam size  $w_i$  is reduced. The insert shows a thin, nonlinear film with incident and transmitted rays of light.

$$E(x, L) \equiv E_T(x) \\ = E_0(x) \exp[i\Phi_0(x)] \exp[-i[n_0 + n_2|E_0(x)|^2]kL]. \quad (2)$$

The far-field distribution of the field over the angular coordinate,  $\theta$ , is found by determining the Fourier transform  $\xi(\theta)$  of the transmitted field,  $E_T(x)$ , and scaling the result by  $1/d$ , where  $d \gg (D, R_{NL})$  is the distance from the film to the far-field region, and

$$\xi(\theta) = \int_{-\infty}^{\infty} dx E_T(x) \exp(ikx\theta). \quad (3)$$

In the ideal case this self-deflection is achieved by using an incident beam with a right-triangular intensity profile<sup>1</sup> (thereby creating a light-induced prism in the beam path) in the form

$$|E(x)|^2 = \begin{cases} |E_m|^2(1 - x/w) & 0 < x < w, \\ 0 & \text{otherwise} \end{cases} \quad (4)$$

the wave front is assumed to be planar,  $\Phi_0 = \text{constant}$ . In the linear case ( $n_2|E_m|^2 = 0$ ) the far electric field is given by  $\xi_L(\theta) = |E_m| \int_0^w dx (1 - x/w)^{1/2} \exp(ikx\theta)^{1/2}$ , and the exact solution, which can be expressed in terms of the Fresnel integrals  $C$  and  $S$ ,<sup>18</sup> is given as

$$\xi_L(\theta) = E_m w \left\{ \frac{i}{\theta} - \left( \frac{\pi}{2\theta^3} \right)^{1/2} [S(\theta^{1/2}) + iC(\theta^{1/2})] e^{i\theta} \right\}, \quad (5)$$

where  $\theta = kw\theta$ . Equation (5) is consistent with the self-deflected component in an expression in Ref. 5 in which a diffraction term is included in the three-dimensional treatment (also constrained by  $\partial E/\partial y = 0$ ). In the case where the nonlinearity of the film is included, substituting Eq. (4) into Eqs. (2) and (3) and noting that  $|E_0(x)|^2$  is linear in  $x$  over the range of the integral, we can use the sifting property of Fourier transforms to show that the linear and nonlinear

profiles are *identical*, except that one is uniformly shifted from the other by an angle  $\theta_{NL}$ :

$$|\xi_{NL}(\theta)| = |\xi_L(\theta - \theta_{NL})|, \quad (6)$$

where

$$\theta_{NL} = -n_2|E_m|^2 L/w = -\phi_{NL} \theta_d/2, \quad (7)$$

$\phi_{NL} = n_2 k L |E_m|^2$  is the maximum phase retardation of the transmitted beam due to the nonlinearity and  $\theta_d = 2/kw$  is the diffraction angle. Equation (7) is consistent with the expression in Ref. 1 for self-bending in the geometric-optics approximation. Below we examine how well this result estimates the self-deflection angle of more realistic (e.g., Gaussian) beams.

At this point we investigate whether the self-deflection effect is altered as the beam is made more nearly symmetric. Thus we now consider an *arbitrary* triangular profile composed of two adjacent right-triangular profiles of different sizes,  $w_1$  and  $w_2$ , but with the same maximum intensity  $|E_m|^2$ . When we apply the sifting property over the intervals  $[0, w_i]$ , we see that two undistorted counter-deflected beams occur in the far field, where each portion of the incident beam is deflected independently:

$$|\xi_{NL}(\theta)|^2 = |\xi_L(\theta - \theta_1) + \xi_L(\theta + \theta_2)|^2, \quad (8)$$

where  $\theta_i = -n_2|E_m|^2 L/w_i$ ,  $i = 1, 2$ . If, for example,  $w_2 \rightarrow 0$ , then the peak intensity at  $\theta_2 \rightarrow -\infty$  diminishes to zero, and the results for a right-triangular profile are recovered.

From Eq. (8) we note that if  $\theta_i$  is larger than the diffraction angle  $\theta_d$ , then the cross term is zero, and the beam is essentially split into two beams. It is therefore meaningful to measure the deflection angle relative to the angular spreading of the beam due to diffraction. This ratio indicates how well the deflected beam profile is resolved from the linear profile. For triangular beams, Eq. (7) gives  $|\theta_{NL}/\theta_d| = |\phi_{NL}/2|$ . The minimum bending required for many applications (e.g., radiation protection and optical bistability) is  $|\theta_{NL}/\theta_d| \sim 1$ . For example, a value of  $|\theta_{NL}/\theta_d| = 5$  may be expected in CdS, in which  $n_2 E_0^2 = 0.15$  was measured at milliwatt power levels ( $< 10$  mW) with a laser tuned near the  $I_2$ -bound excitation resonance at 487 nm in samples 5–20  $\mu\text{m}$  thick.<sup>13</sup>

Although  $\theta_{NL}/\theta_d$  does not depend on the beam size explicitly, these results are valid only when the beam size is large enough to satisfy the thinness condition [Eq. (1)]. In the

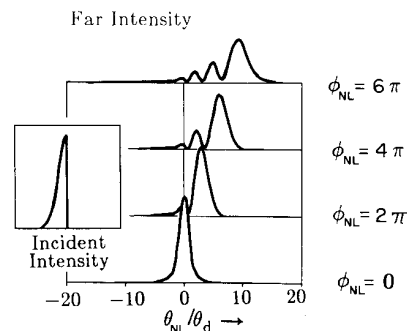


Fig. 2. Self-deflection due to a semi-Gaussian intensity profile for nonlinear parameter  $\phi_{NL} = 2\pi j$ ,  $j = 0, 1, 2, 3$ . The deflection angle  $\theta_{NL}$  of the largest peak is given by Eq. (7). The number of subpeaks is equal to  $j$ .

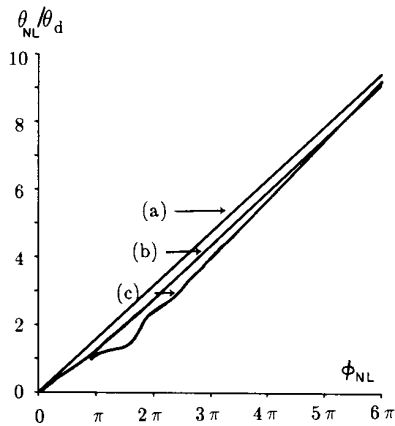


Fig. 3. The deflection angle of the peak intensity in the far field versus the nonlinear parameter  $\phi_{NL}$ . Incident intensity profiles are (a) right-triangular, (b) semi-Gaussian, and (c) symmetric Gaussian.

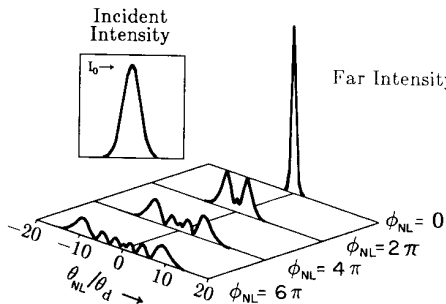


Fig. 4. Counter-self-deflection due to a symmetric Gaussian intensity profile for different nonlinear parameters;  $\phi_{NL} = 2\pi j$ , where  $j = 0, 1, 2, 3$ .

following numerical analyses, this condition is always satisfied because we assume that  $kL \rightarrow 0$  and  $\phi_{NL} = \text{constant}$ . Furthermore, if the beam power is fixed but its size is reduced (focused), as in Fig. 1, then we find that  $\theta_{NL}/\theta_d$  increases as  $w^{-1}$ . The numerical data verify the analytical result expressed in Eq. (8).

The profiles considered above were presented to demonstrate ideal self-deflection effects; we must now consider more realistic beam profiles, in particular, Gaussian ones. In this case, to obtain the strongest self-deflection angle for a given beam power, half the beam is obscured so that it resembles a right-triangular profile:

$$E_0(x) = \begin{cases} E_m \exp[-(x/w)^2] & x > 0 \\ 0 & \text{otherwise} \end{cases} \quad (9)$$

An analytical solution for this beam inserted into Eqs. (2) and (3) cannot be found; hence we treat the problem numerically. The far intensity profile, as shown in Fig. 2, is symmetric in the linear case ( $\phi_{NL} = 0$ ). The nonlinear case yields a strong peak whose deflection angle increases as  $\phi_{NL}$  (see also Fig. 3). In addition there are also some lesser deflected subpeaks, whose number is approximately  $j \approx \phi_{NL}/2\pi$ . Because the incident beam profile is quasi-triangular, we may expect to approximate the angle of deflection by Eq. (7). In fact, Fig. 3 verifies that this approximation is excellent. The agreement is somewhat surprising since we may

have expected the semi-Gaussian result to diverge continuously from the right-triangular result as the intensity increased. Because the right-triangular self-deflection angle is the upper limit (for a given peak intensity and intensity gradient), the semi-Gaussian beam profile therefore produces a nearly maximum self-deflection angle. We believe that by using a single retroreflecting mirror in a far-field area, this effect can be used<sup>4</sup> to observe resonatorless optical bistability and switching similar, to some extent, to the self-focusing bistability.<sup>4,19</sup>

From the point of view of these (not quite expected) results, it is interesting to look into the case of a symmetric (unobscured) Gaussian profile. In the intermediate region, between the film and the far field, self-(de)focusing of the beam will occur<sup>7,8</sup> when  $\phi_{NL}$  is nonzero. The common assumption in the theory of self-focusing is that the incident Gaussian beam induces a quasi-parabolic (in our case, cylindrical) lens in the film, causing the far-field beam to remain somewhat Gaussian in nature. However, in spite of these expectations, our numerical results (Fig. 4) show that, instead of a self-(de)focused nearly Gaussian beam, there are two strongly counter-self-deflected beams in the far field, with almost no energy propagating along the central axis. This result is quite surprising as well. Indeed, although self-focusing was seen in many experiments (with three-dimensional beams) almost always to be accompanied with surrounding rings, there is also a strong component propagating along the central axis. In the two-dimensional case, according to our calculations, the beam energy is deflected away from the axis, as in Fig. 4, rather than remaining localized on the axis. This counter-self-deflection action can be viewed in the context of self-bending, resulting from two adjacent semi-Gaussian prisms (each of which deflects its portion of the beam).

In conclusion, we have demonstrated that the self-deflection effect can be expected from thin nonlinear films of materials now in existence. We compared the ideal self-deflection case (with a right-triangular beam profile) with a more realistic semi-Gaussian beam and found that the self-deflection angles are approximately the same. We also observed that, for a symmetric beam, deflection dominates over self-focusing. We expect that materials such as CdS, quantum-well structures, and liquid crystals will be useful in applications of the self-deflection effect, such as radiation protection, optical switching and bistability, optical limiting, and nonlinear-optical coupling devices.

## ACKNOWLEDGMENT

This research was supported by the U.S. Air Force Office of Scientific Research.

## REFERENCES AND NOTES

1. A. E. Kaplan, JETP Lett. **9**, 33 (1969) [Pis'ma Zh. Eksp. Teor. Fiz. **9**, 58 (1969)].
2. M. S. Brodin and A. M. Kamuz, JETP Lett. **9**, 351 (1969) [Pis'ma Zh. Eksp. Teor. Fiz. **9**, 577 (1969)].
3. L. I. Gudzenko, C. D. Kaitmazov, A. A. Medvedev, and E. I. Schklovsky, Lebedev Inst. Phys. Brief Commun. Phys. **1**, 64 (1970, in Russian).
4. A. E. Kaplan, Opt. Lett. **6**, 360 (1981).

5. J. A. Hermann, *Opt. Commun.* **62**, 367 (1987); *Opt. Quantum Electron.* **19**, 169 (1987).
6. P. L. Kelley, *Phys. Rev. Lett.* **15**, 1005 (1965); S. A. Akhmanov, R. V. Khokhlov, and A. P. Sukhorukov, in *Laser Handbook*, F. T. Arecchi and E. O. Schulz-Dubois, eds. (North-Holland, Amsterdam, 1972), Vol. 2, p. 1151; Y. R. Shen, *Rev. Mod. Phys.* **48**, 1 (1976).
7. P. D. McWane, *Nature* **211**, 1081 (1966).
8. A. E. Kaplan, *Radiophys. Quantum Electron.* **12**, 692 (1969) [*Izv. Vyssh. Ucheb. Zaved. Radiofiz.* **12**, 869 (1969)]; F. S. Felber, *Appl. Phys. Lett.* **36**, 723 (1980).
9. T. F. Boggess, S. C. Moss, I. W. Boyd, and A. L. Smirl, *Opt. Lett.* **9**, 291 (1984); T. F. Boggess, A. L. Smirl, S. C. Moss, I. W. Boyd, and E. W. Van Stryland, *IEEE J. Quantum Electron.* **QE-21**, 488 (1985).
10. J. A. Hermann, *J. Opt. Soc. Am. B* **1**, 729 (1984).
11. G. A. Swartzlander, Jr., M. S. thesis (Purdue U., West Lafayette, Indiana, 1985) (unpublished).
12. D. A. B. Miller, D. S. Chemla, D. J. Eilenberger, P. W. Smith, A. C. Gossard, and W. T. Tsang, *Appl. Phys. Lett.* **41**, 679 (1982); D. S. Chemla and D. A. B. Miller, *J. Opt. Soc. Am. B* **2**, 1155 (1985).
13. M. Dagenais and H. G. Winful, *Appl. Phys. Lett.* **44**, 574 (1984); M. Dagenais and W. F. Sharfin, *J. Opt. Soc. Am. B* **2**, 1179 (1985).
14. I. C. Khoo, *Phys. Rev. A* **25**, 1636 (1982).
15. A. Ashkin, J. M. Dziedzic, and P. W. Smith, *Opt. Lett.* **7**, 276 (1982); P. W. Smith, P. J. Maloney, and A. Ashkin, *Opt. Lett.* **7**, 347 (1982).
16. S. Friberg and P. W. Smith, *IEEE J. Quantum Electron.* **QE-23**, 2089 (1987).
17. I. C. Khoo, R. R. Michael, T. H. Liu, G. Finn, and A. E. Kaplan, *Proc. Soc. Photo-Opt. Instrum. Eng.* **613**, 43 (1986).
18. We use the following definition of the Fresnel integrals:  $S(u) = (1/\sqrt{2\pi}) \int_0^{u^2} [\sin(t)/\sqrt{t}] dt$  and  $C(u) = (1/\sqrt{2\pi}) \int_0^{u^2} [\cos(t)/\sqrt{t}] dt$ . [See *Handbook of Mathematical Functions*, M. Abramowitz and I. A. Stegun, eds. (Dover, New York, 1972).]
19. J. E. Bjorkholm, P. W. Smith, W. J. Tomlinson, and A. E. Kaplan, *Opt. Lett.* **6**, 345 (1981); I. C. Khoo, P. J. Yan, T. H. Liu, S. Shepard, and J. Y. Hou, *Phys. Rev. A* **29**, 2756 (1984); K. Tai, M. M. Gibbs, N. Peyghambarian, and A. Mysyrowicz, *Opt. Lett.* **10**, 220 (1985); M. Le Berre, E. Ressayre, A. Tallet, K. Tai, and H. M. Gibbs, *IEEE J. Quantum Electron.* **QE-21**, 1404 (1985).